

Application of carbonized cellulose-based catalyst in nitrobenzene hydrogenation

Á. Prekob^{a,*}, V. Hajdu^a, G. Muránszky^a, B. Fiser^{a,b}, A. Sycheva^c, T. Ferenczi^d,
B. Viskolcz^a, L. Vanyorek^a

^a Institute of Chemistry, University of Miskolc, 3515, Miskolc-Egyetemváros, Hungary

^b Ferenc Rákóczi II, Transcarpathian Hungarian Institute, 90200, Beregszász, Transcarpathia, Ukraine

^c MTA-ME Materials Science Research Group, University of Miskolc, 3515, Miskolc-Egyetemváros, Hungary

^d Institute of Metallurgy, University of Miskolc, 3515, Miskolc-Egyetemváros, Hungary

ARTICLE INFO

Article history:

Received 9 April 2020

Received in revised form

2 July 2020

Accepted 3 July 2020

Available online 24 July 2020

Keywords:

Cellulose beads

Carbonization

Aniline

Characterization

Catalysis

ABSTRACT

Carbonized cellulose catalyst support was prepared and decorated with 5 wt% Pd nanoparticles using an impregnation method. According to the SEM images, the carbonized cellulose catalyst support kept its original fibrous structure with an average diameter of 200 nm, owing to the carbonization of the cellulose fibers. The surface of the formed carbon fibers is richly coated by palladium with even coverage. The particles can be divided into two groups within which the average diameter is either 5 nm, or 20–70 nm. TGA method was used to measure the amount of the remained carbon, which was 31.71 wt%. The FTIR spectrum shows the presence of oxygen containing functional groups on the surface of the support, which are hydroxyl groups. XRD method was used to determine the phases of Pd on the support where elemental Pd was detected which confirms the success of the activation step. The catalyst was tested in nitrobenzene hydrogenation in methanolic solution as a model reaction for nitroarene hydrogenation, meanwhile the temperature dependence of the reaction was also examined. Catalytic tests were carried out at four different temperatures (283–323 K) and constant hydrogen pressure (20 bar). The highest conversion (>99%) has been reached at 303 K and 20 bar. The corresponding activation energy was calculated by non-linear regression based on Arrhenius plot, and it was 24.16 ± 0.8 kJ/mol. All in all, the granulated cellulose beads are ideal starting points for carbon based catalyst supports.

© 2020 The Author(s). Published by Elsevier Ltd. This is an open access article under the CC BY license (<http://creativecommons.org/licenses/by/4.0/>).

1. Introduction

Hydrogenation of nitro compounds is widely studied [1–6], because the produced amines involved in various important applications such as pharmaceuticals [7–9], biosensing [10], synthesis of dyes [11], and in removal processes [12]. A wide range of catalysts such as AuPd/TiO₂ bimetallic catalyst (E_a : 37 kJ/mol), Pt/γ-Al₂O₃ (E_a : 37 kJ/mol), and Ru/FeOx (E_a : 33 kJ/mol) have been tested in nitrobenzene hydrogenation to produce aniline [13–15]. However, carbon based catalyst supports are more often used in heterogeneous catalysis [16–18] because of their excellent properties [19], not to

mention that they can be prepared by carbonization from almost any available carbon source [20–22]. Furthermore, carbonized catalysts show better results than non-carbonized materials in the hydrogenation of nitroarenes [23].

Cellulose could be one of the most promising material for support preparation due to the fact that it is available in large quantities in nature, biodegradable, highly functionalized, nontoxic and thus, excellent for sustainable carbon support production [24,25]. It has many applications within which its shape, structure, particle size, and orientation is adapted accordingly [26–30]. Cellulose based Pd/Co bimetallic catalyst was tested in nitrobenzene reduction by using H₂O/EtOH as solvent and NaBH₄ as reducing agent [31]. Furthermore, modified cellulose based catalyst was applied in the hydrogenation of different nitroarenes [32].

Nitrobenzene hydrogenation could occur through a direct or a condensation route [37]. However, regardless of the route, the reaction is highly sensitive to temperature which makes the

* Corresponding author.

E-mail addresses: prekob.a@gmail.com (Á. Prekob), kemwiki@uni-miskolc.hu (V. Hajdu), kemmug@uni-miskolc.hu (G. Muránszky), fiser@uni-miskolc.hu (B. Fiser), a.sycheva@uni-miskolc.hu (A. Sycheva), femft@uni-miskolc.hu (T. Ferenczi), bela.viskolcz@uni-miskolc.hu (B. Viskolcz), kemvanyi@uni-miskolc.hu (L. Vanyorek).

examination of temperature dependence necessary in case of every catalyst development process [38].

In this study, carbonized cellulose sphere based Pd catalyst has been prepared, characterized, and tested in nitrobenzene hydrogenation as a simple model reaction for the hydrogenation of nitro compounds. Simple handling of the catalyst and separation from the medium is possible with the applied support. Furthermore, the fibrous structure with the lack of macro and meso porosity accelerates the mass transport during reaction. Moreover, the developed catalyst and the preparation process is sustainable, because the method is simple, and the applied support is very common and available in large quantities.

2. Experimental

2.1. Materials

Cellulose beads ("Mavicell") were purchased from *Magyar Viscosagyár*. According to the product description, Mavicell is a 100% cellulose based, semi-synthetic spherical material. Nitrogen gas was used as inert atmosphere (*Messer 4.5*). The Pd nanoparticles were prepared by using Pd(II) nitrate dihydrate (*Sigma-Aldrich*, $\text{Pd}(\text{NO}_3)_2 \times 2\text{H}_2\text{O}$, 40% Pd basis) as a precursor with water as solvent, and hydrogen gas (*Messer 4.5*) for the activation.

2.2. Catalyst preparation

The cellulose beads were carbonized in nitrogen atmosphere at 1,173 K for 1 h. After the carbonization 1 g carbonized cellulose was impregnated with the Pd nitrate solution (0.125 g $\text{Pd}(\text{NO}_3)_2 + 70$ ml H_2O) for 30 min. Thereafter, the water was removed by vacuum evaporation. The catalyst was dried at 378 K overnight. First, the impregnated beads were calcined at 673 K in nitrogen atmosphere for 30 min, then activated in hydrogen atmosphere at the same temperature for 1 h.

2.3. Characterization techniques of the catalyst

The carbonization process was monitored by using a Tarsus TG 209 microbalance. During this, the sample was heated by using a 10 K/min heating speed from 308 K to 1,173 K. The carbonization was carried out in nitrogen atmosphere with a continuous 20 ml/min flow velocity. As the measurement was carried out in inert atmosphere after the second weight loss of the sample the remained material is carbon.

The functional groups of the sample were detected by using a Bruker Vertex 70 type instrument. The sample was examined in potassium-bromide pellets (5 mg sample in 250 mg KBr) with 16 s^{-1} scanning velocity and 4 cm^{-1} resolution.

The SEM images were made by a Hitachi 4800 instrument where the samples were fixed with carbon tape rubber. The SEM instrument was equipped with an EDX detector which was used to carry out the elemental analysis of the samples.

The type of the crystalline phases of the Pd nanoparticles was determined by using a Rigaku Miniflex instrument with $\text{Cu-K}\alpha$ source.

The catalyst was tested in nitrobenzene hydrogenation using a Büchi Uster Picoclave reactor with continuous mixing, constant and controlled hydrogen flow, and controlled pressure and temperature values.

The product samples of the test reactions were examined by gas chromatography (Agilent 7890A coupled with Agilent 5975C Mass Selective detector). Analytical standards were provided by Dr. Ehrenstorfer and Sigma Aldrich (aniline, nitrobenzene,

nitrosobenzene, azoxybenzene, dicyclohexylamine, *o*-toluidine, cyclohexylamine and *n*-methylaniline).

2.4. Catalytic tests

For each catalytic test 0.2 g 5 wt% Pd containing catalyst and 150 ml 0.25 mol/L nitrobenzene/methanol solution were used. The system was continuously mixed with 1,000 1/min rotation speed. The tests were carried out at 283 K, 293 K, 303 K, and 323 K, under 20 bar hydrogen pressure. During the hydrogenation process the reactions were monitored and samples were taken at 5, 10, 15, 30, 60, 120, 180, and 240 min. The samples were examined by using gas chromatography (GC).

3. Results and discussion

3.1. Properties of the catalyst

3.1.1. Results of the thermogravimetric analysis (TGA) and Fourier-transform infrared spectroscopy (FTIR)

TGA measurement was applied to monitor the carbonization process (Fig. 1. A). During the process two significant weight loss were detected, within which the first occurred between 321 K and 482 K and it can be associated with the loss of the water content of the samples. The second weight loss have taken place between 482 K and 664 K and it can be linked to the carbonization of the cellulose. The total weight loss was 68.29 wt% and thus, only 31.71 wt% of the initial weight of the cellulose converted to carbon in the carbonization process.

FTIR spectroscopy was used to determine the functional groups of the initial and carbonized cellulose beads (Fig. 1. B). The spectra are very similar for both cases. Three main peaks have been identified at $1,635 \text{ cm}^{-1}$, $3,238 \text{ cm}^{-1}$, and $3,449 \text{ cm}^{-1}$ wavenumbers which indicates the presence of C=C bonds, -CH groups, and hydroxyl groups, respectively.

3.1.2. Results of the scanning electron microscopy (SEM) and X-ray diffraction (XRD) analysis

SEM images were taken to examine the structure of the support and the Pd nanoparticles. It can be seen that the support kept the fibrous structure after carbonization (Fig. 2. A). The diameter of the fibers is ~200 nm. The presence of the Pd nanoparticles on the surface of the support have been verified with high dispersity. There are smaller nanoparticles and bigger aggregates with an average diameter of 5 nm and 20–70 nm, respectively (Fig. 2. B). EDX spectroscopy was used to carry out the elemental analysis of the samples (Fig. 2. C). It also confirmed the presence of Pd and C. Furthermore, small amount of Mg, Al, and S were also identified, which are probably filler materials in the cellulose beads. XRD measurement was used to determine the type of the crystalline phases of the Pd nanoparticles (Fig. 2. D). The (111), (200), and (220) Miller-indexed crystal planes have been identified in the samples at 40, 47, and 68 2θ degrees, respectively. Thus, the total amount of palladium is present in elemental (metallic) state which confirms that, the reduction step of the catalyst activation was efficient.

According to BET measurements, the specific surface area (SSA) of the catalyst is $289.70 \text{ m}^2/\text{g}$ (Table 1). For comparison, the carbonized beads without metal and the catalyst after its application, but without regeneration have also been measured. The SSA of the carbonized cellulose beads is almost two times as smaller as the catalyst. Furthermore, the pore diameter of the carbonized cellulose is also smaller (1.90 nm) compare to the final catalytic system. After using it, the SSA of the catalyst have decreased significantly (<10% of the original surface). Moreover, the average pore diameter of the catalyst has also dropped from 2.05 nm to 1.89 nm.

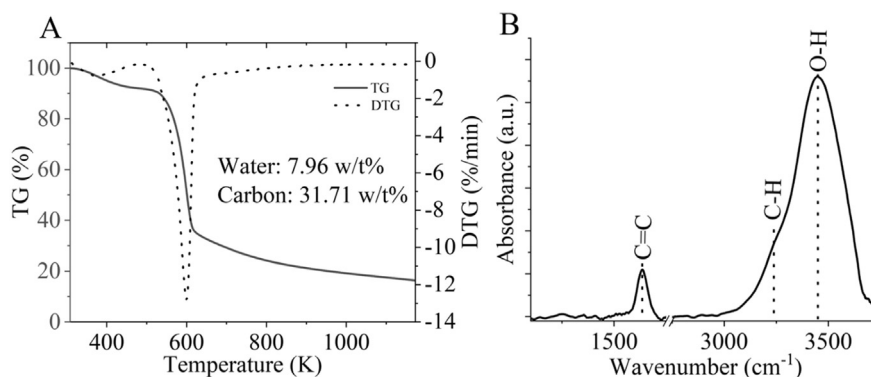


Fig. 1. TGA (A) measurement of the initial and FTIR (B) spectrum of the carbonized cellulose beads.

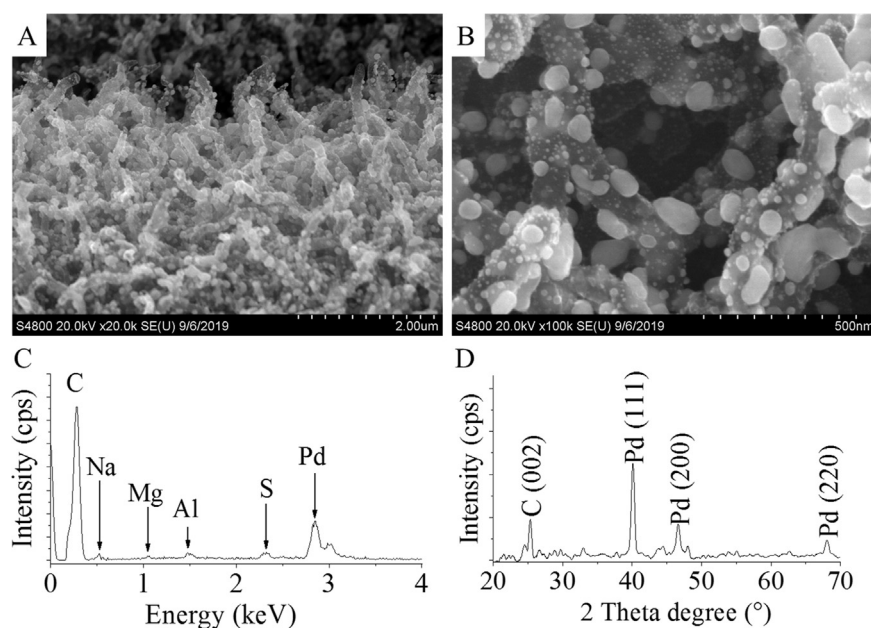


Fig. 2. SEM images (A, B), EDX spectra (C) and XRD diffractogram (D) of the final catalyst.

Table 1

Specific surface area (SSA) and average pore diameter (APD) of the catalyst (5% w/w Pd-CC) and the support, where CC is carbonized cellulose.

	5% w/w Pd-CC	5% w/w Pd-CC (after using it, but without regeneration)	CC
SSA (m ² /g)	289.70	22.21	148.59
APD (nm)	2.05	1.89	1.90

3.2. Catalytic performance

The prepared catalyst has been tested in nitrobenzene hydrogenation. The experiments have been carried out at four different temperatures (283, 293, 303 and 323 K), and the corresponding conversions were calculated (Fig. 3. A). The nitrobenzene conversion is highly depending on the temperature. At 323 K it was almost 100%, meanwhile at 283 K only 64% was reached.

The selectivity was also measured for the product, intermediates, and by-product (Fig. 3. B). It can be seen, that the ~100% nitrobenzene conversion was reached only at 323, so the rate of the intermediates was higher on lower temperatures. Increasing the temperature gradually decreased their concentration and

increased the aniline quantity up to 91.15%. However, the slow increase of the N-methylaniline.

Our results were compared to other Pd contained catalyst used by other researchers in nitrobenzene hydrogenation (Table 2.). To compare catalysts with different Pd content, turnover number (TON) was calculated. However, the pressure, temperature, solution concentration and hydrogenation time values are very different in every paper, so this method provides only an approximate comparison.

Based on the nitrobenzene concentration of the samples, the reaction rate constants (*k*) were also calculated at different temperatures (283 K, 293 K, 303 K and 323 K) by using a non-linear regression method (Fig. 4 A, Table 3.) [39].

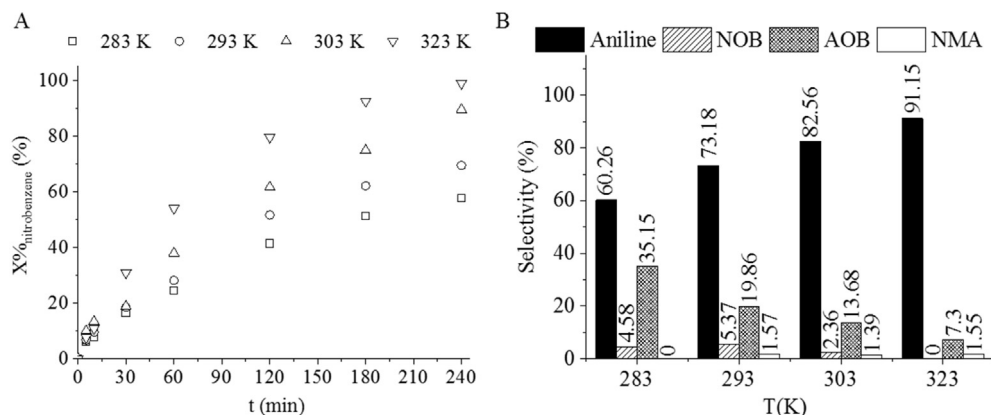


Fig. 3. Nitrobenzene conversion (X%) vs. time of hydrogenation (A) and selectivity on different temperatures (B).

By applying the natural logarithm of reaction rate constants, the activation energy was also calculated by using the Arrhenius plot. The (k) rate constants were plotted as a function of the temperature, and the activation energy has been calculated (Fig. 4 B). The activation energy was 24.16 kJ/mol.

Two intermediates, nitrosobenzene (NOB) and azoxybenzene (AOB) have also been identified in the reaction media. The hydrogenation of these species to aniline was enhanced by increasing the reaction temperature, but these were not converted completely, as after 4 h of reaction they can still be found (Fig. 5). Only one by-

Table 2
Comparison of 5% Pd/CC catalyst with other Pd contained catalysts.

Reference	Catalyst	W_{cat} (g)	p (bar)	T (K)	C_{NB} (mol L ⁻¹)	t (min)	TON (mol _{AN} /mol _{Pd})
This paper	5% Pd/CC	0.2	20	323	0.250	240	360.19
[33]	1% Pd/Al ₂ O ₃	80	15	423	0.812	240	92.93
[34]	5.22% Pd/AC	0.025	10	313	0.326	15	295.97
[34]	4.24% Pd/Al ₂ O ₃	0.025	10	313	0.326	15	77.94
[34]	5.28% Pd/MWCNT	0.025	10	313	0.326	15	281.09
[35]	5% Pd/ γ -Fe ₂ O ₃	0.2	20	303	0.125	240	382.05
[36]	1.5% Pd/C-PVC	0.2	5	323	0.100	30	350.47

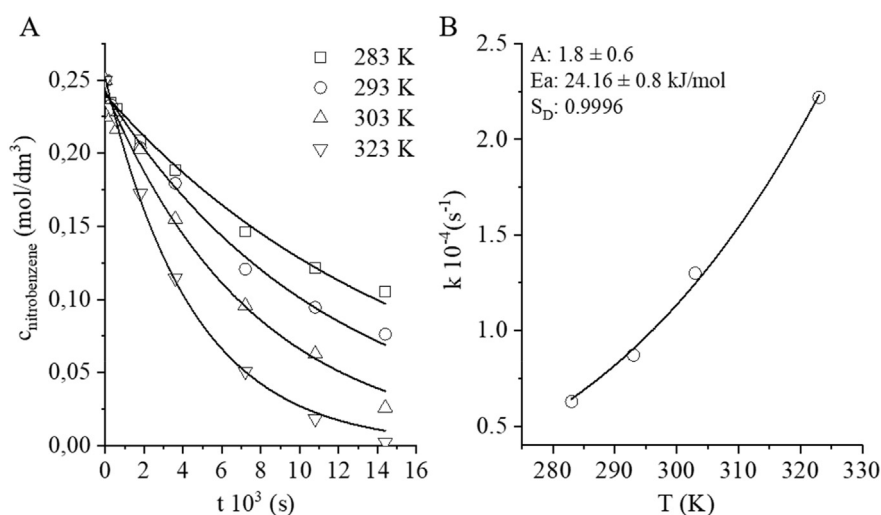


Fig. 4. Conversion values of nitrobenzene hydrogenation at different temperatures (A) and the corresponding Arrhenius plot (B).

Table 3
Reaction rate constants of nitrobenzene hydrogenation at different temperatures.

Temperature (K):	283	293	303	323
Reaction rate constant (s ⁻¹):	6.283×10^{-5}	8.714×10^{-5}	1.303×10^{-4}	2.224×10^{-4}
SD:	3.33×10^{-6}	3.93×10^{-6}	8.00×10^{-6}	7.71×10^{-6}

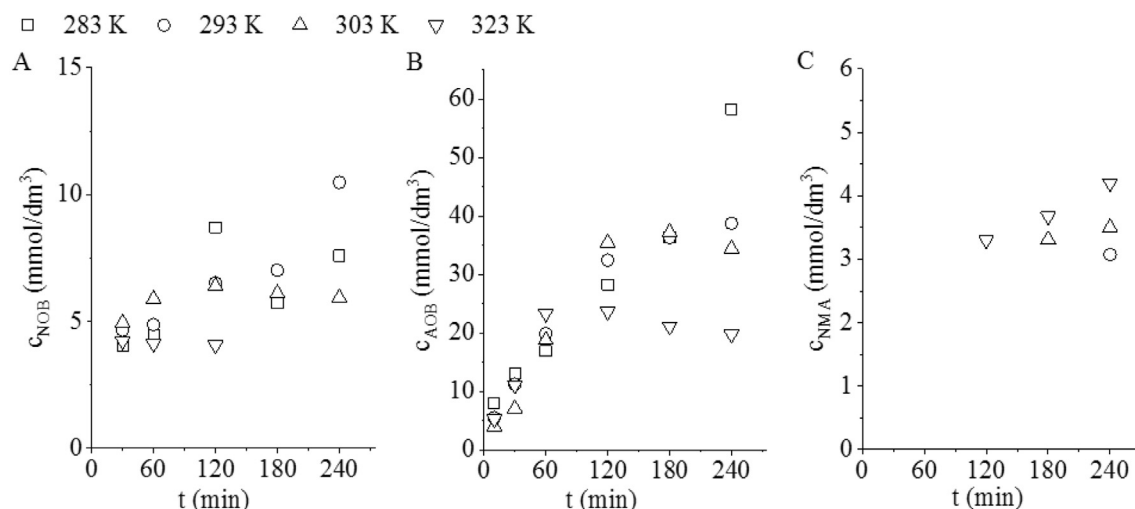


Fig. 5. Concentration of nitrosobenzene (A) and azoxybenzene (B) and N-methylaniline (C) vs. time of hydrogenation at different temperature values.

product, N-methylaniline (NMA) was formed at higher temperature (293 K, 303 K and 323 K) values, but in small concentration ($4,5 > \text{mmol/dm}^3$). By decreasing the reaction temperature, the reaction rate was also lower, and thus the concentrations of the intermediates are higher. Although, N-methylaniline was not formed at 283 K.

The hydrogenation reaction was repeated at 323 K four times to check the regenerative capacity of the catalyst (Fig. 6). Between each test, the activation process was repeated with the same parameters, as mentioned before (30 min in nitrogen and 30 min in hydrogen atmosphere at 673 K). The regeneration of the catalyst was not complete, but the conversion was still reasonable, as it is dropped from ~100% to 82% at the third attempt.

It is a difficult job to compare our results with others in literature. For better comparison, the same parameters and Pd content were used in two of our earlier papers [35,40]. Comparing to our 5 wt% Pd N-doped carbon nanotube/zeolite composite catalyst the cellulose based catalyst provided higher specific surface area ($15 \text{ m}^2/\text{g}$ for zeolite composite, $289,70 \text{ m}^2/\text{g}$ for carbonized

cellulose) and fibrous structure with low porosity for faster mass transport [40].

In case of our 5 wt% Pd/maghemite magnetic catalyst, the preparation was more complex (including a combustion step), more reagents were necessary, and was more difficult to handle due to its powder form [35].

4. Conclusion

In this paper cellulose beads were carbonized in inert atmosphere, then decorated with 5 w/w% Pd. The catalyst was characterized by TGA, FTIR, SEM, EDX, and XRD methods. As a result, a carbonized fibrous structured catalyst support was prepared and decorated with Pd. The fibers were present with an average diameter of 200 nm. The support surface was abundantly coated with Pd nanoparticles (average diameters are 5 nm, and between 20 and 70 nm). The catalyst was activated by using hydrogen atmosphere and the activation was confirmed by XRD measurements. After the characterization of the catalyst, it was tested in nitrobenzene hydrogenation at four different temperatures under 20 bar hydrogen pressure. The catalyst was applicable in the procedure aniline synthesis and it could reach almost 100% nitrobenzene conversion at 323 K after 4 h. The regeneration capacity of the developed system is also reasonable, as the conversion only dropped to 82% at the fourth attempt of use.

CRediT authorship contribution statement

Á. Prekob: Conceptualization, Investigation, Writing - original draft. V. Hajdu: Investigation. G. Muránszky: Conceptualization, Validation. B. Fiser: Validation, Writing - review & editing, Validation. T. Ferenczi: Validation. B. Viskolcz: Resources, Supervision. L. Vanyorek: Conceptualization, Supervision.

Declaration of Competing Interest

The authors declare that they have no known competing financial interests or personal relationships that could have appeared to influence the work reported in this paper.

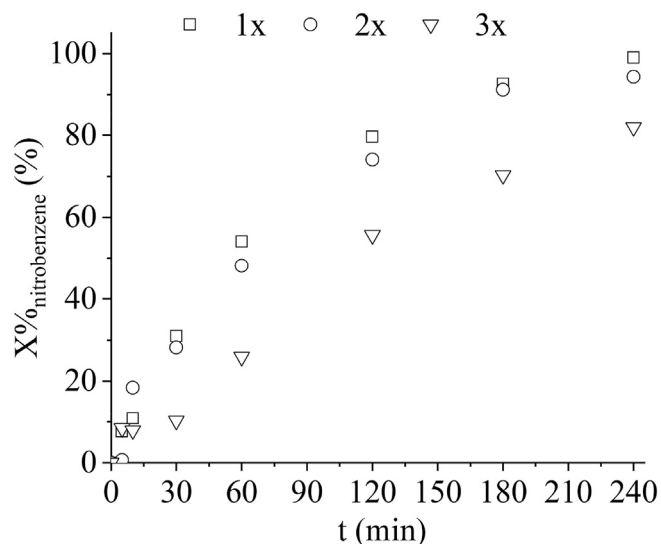


Fig. 6. Nitrobenzene conversion (X%) vs. time of hydrogenation at 323 K during the first (1x), second (2x) and third (3x) use of the catalyst.

Acknowledgments

This research was supported by the European Union and the Hungarian State, co-financed by the European Regional Development Fund in the framework of the GINOP-2.3.4-15-2016-00004 project, aimed to promote the cooperation between the higher education and the industry.

References

- [1] Y. Aubakirov, L. Sassykova, S. Subramanian, K. Bhaskar, U. Otzhan, M. Amangeldi, T. Abildin, A. Zhumakanova, A. Zhussupova, M. Zharkyn, Hydrogenation of aromatic nitro-compounds of a different structure in a liquid phase, *J. Chem. Technol. Metall.* 54 (2019) 522–530.
- [2] L. Huang, Y. Lv, S. Wu, P. Liu, W. Xiong, F. Hao, H. Luo, Activated carbon supported bimetallic catalysts with combined catalytic effects for aromatic nitro compounds hydrogenation under mild conditions, *Appl. Catal. Gen.* 577 (2019) 76–85, <https://doi.org/10.1016/j.apcata.2019.03.017>.
- [3] L. Lang, Z. Pan, J. Yan, Ni-Au alloy nanoparticles as a high performance heterogeneous catalyst for hydrogenation of aromatic nitro compounds, *J. Alloys Compd.* 792 (2019) 286–290, <https://doi.org/10.1016/j.jallcom.2019.03.323>.
- [4] O. Verho, K.P. Gustafson, A. Nagendiran, C.-W. Tai, J.-E. Bäckvall, Mild and selective hydrogenation of nitro compounds using palladium nanoparticles supported on amino-functionalized mesocellular foam, *ChemCatChem* 6 (2014) 3153–3159, <https://doi.org/10.1002/cctc.201402488>.
- [5] M. Ueno, Y. Morii, K. Uramoto, H. Oyamada, Y. Mori, S. Kobayashi, Catalytic flow hydrogenation of aromatic nitro compounds using polysilane-supported palladium, *J. Flow Chem.* (2014), <https://doi.org/10.1556/JFC-D-14-00024>.
- [6] P. Zhou, D. Li, S. Jin, S. Chen, Z. Zhang, Catalytic transfer hydrogenation of nitro compounds into amines over magnetic graphene oxide supported Pd nanoparticles, *Int. J. Hydrogen Energy* 41 (2016) 15218–15224, <https://doi.org/10.1016/j.ijhydene.2016.06.257>.
- [7] G.W. Lamb, F.A. Al Badran, J.M.J. Williams, S.T. Kolaczowski, Production of pharmaceuticals: amines from alcohols in a continuous flow fixed bed catalytic reactor, *Chem. Eng. Res. Des.* 88 (2010) 1533–1540, <https://doi.org/10.1016/j.cherd.2010.04.005>.
- [8] Z. Feng, K. Odelius, G.K. Rajarao, M. Hakkarainen, Microwave carbonized cellulose for trace pharmaceutical adsorption, *Chem. Eng. J.* 346 (2018) 557–566, <https://doi.org/10.1016/j.cej.2018.04.014>.
- [9] H. Ullah, F. Wahid, H.A. Santos, T. Khan, Advances in biomedical and pharmaceutical applications of functional bacterial cellulose-based nanocomposites, *Carbohydr. Polym.* 150 (2016) 330–352, <https://doi.org/10.1016/j.carbpol.2016.05.029>.
- [10] T.U.H. Shah, M.H. Tahir, M.S. Ahmad, A. ur Rahman, M.A. kamran, H. Liu, Stimuli-responsive fluorescent hyperbranched poly(amido amine)s for biosensing applications, *Eur. Polym. J.* 124 (2020), <https://doi.org/10.1016/j.eurpolymj.2020.109486>.
- [11] S. Benkhaya, S. Mrabet, A. El Harfi, Classifications, properties, recent synthesis and applications of azo dyes, *Heliyon* 6 (2020), <https://doi.org/10.1016/j.heliyon.2020.e03271>.
- [12] C.N. Okonkwo, J.J. Lee, A. De Vylder, Y. Chiang, J.W. Thybaut, C.W. Jones, Selective removal of hydrogen sulfide from simulated biogas streams using sterically hindered amine adsorbents, *Chem. Eng. J.* 379 (2020), <https://doi.org/10.1016/j.cej.2019.122349>.
- [13] R. Qu, M. Macino, S. Iqbal, X. Gao, Q. He, G. Hutchings, M. Sankar, Supported bimetallic AuPd nanoparticles as a catalyst for the selective hydrogenation of nitroarenes, *Nanomaterials* 8 (2018) 690, <https://doi.org/10.3390/nano8090690>.
- [14] J. Peureux, M. Torres, H. Mozzanega, A. Giroir-Fendler, J.-A. Dalmon, Nitrobenzene liquid-phase hydrogenation in a membrane reactor, *Catal. Today* 25 (1995) 409–415, [https://doi.org/10.1016/0920-5861\(95\)00128-3](https://doi.org/10.1016/0920-5861(95)00128-3).
- [15] R. Easterday, O. Sanchez-Felix, Y. Losovyj, M. Pink, B.D. Stein, D.G. Morgan, M. Rikitin, V.Y. Doluda, M.G. Sulman, W.E. Mahmoud, A.A. Al-Ghamdi, L.M. Bronstein, Design of ruthenium/iron oxide nanoparticle mixtures for hydrogenation of nitrobenzene, *Catal. Sci. Technol.* 5 (2015) 1902–1910, <https://doi.org/10.1039/C4CY01277A>.
- [16] F. Zhao, Y. Ikushima, M. Arai, Hydrogenation of nitrobenzene with supported platinum catalysts in supercritical carbon dioxide: effects of pressure, solvent, and metal particle size, *J. Catal.* 224 (2004) 479–483, <https://doi.org/10.1016/j.jcat.2004.01.003>.
- [17] F. Zhao, R. Zhang, M. Chatterjee, Y. Ikushima, M. Arai, Hydrogenation of nitrobenzene with supported transition metal catalysts in supercritical carbon dioxide, *Adv. Synth. Catal.* 346 (2004) 661–668, <https://doi.org/10.1002/adsc.200303230>.
- [18] M.C. Macías Pérez, C. Salinas Martínez De Lecea, A. Linares Solano, Platinum supported on activated carbon cloths as catalyst for nitrobenzene hydrogenation, *Appl. Catal. Gen.* 151 (1997) 461–475, [https://doi.org/10.1016/S0926-860X\(96\)00303-1](https://doi.org/10.1016/S0926-860X(96)00303-1).
- [19] C. Wang, V. Murugadoss, J. Kong, Z. He, X. Mai, Q. Shao, Y. Chen, L. Guo, C. Liu, S. Angaiah, Z. Guo, Overview of carbon nanostructures and nanocomposites for electromagnetic wave shielding, *Carbon N. Y.* 140 (2018) 696–733, <https://doi.org/10.1016/j.carbon.2018.09.006>.
- [20] K. Yang, J. Peng, C. Srinivasakannan, L. Zhang, H. Xia, X. Duan, Preparation of high surface area activated carbon from coconut shells using microwave heating, *Bioresour. Technol.* 101 (2010) 6163–6169, <https://doi.org/10.1016/j.biortech.2010.03.001>.
- [21] Z. Hu, M.P. Srinivasan, Y. Ni, Preparation of mesoporous high-surface-area activated carbon, *Adv. Mater.* 12 (2000) 62–65, [https://doi.org/10.1002/\(SICI\)1521-4095\(200001\)12:1<62::AID-ADMA62>3.0.CO;2-B](https://doi.org/10.1002/(SICI)1521-4095(200001)12:1<62::AID-ADMA62>3.0.CO;2-B).
- [22] P. Ariyadejwanich, W. Tanthapanichakoon, K. Nakagawa, S.R. Mukai, H. Tamon, Preparation and characterization of mesoporous activated carbon from waste tires, *Carbon N. Y.* 41 (2003) 157–164, [https://doi.org/10.1016/S0008-6223\(02\)00267-1](https://doi.org/10.1016/S0008-6223(02)00267-1).
- [23] M.Y. Rikitin, V.Y. Doluda, A.Y. Tereshchenkov, G.N. Demidenko, N.V. Lakina, V.G. Matveeva, M.G. Sul'man, E.M. Sul'man, Investigating the catalytic hydrogenation of nitrobenzene in supercritical carbon dioxide using Pd-containing catalysts, *Catalogue Index* 7 (2015) 1–5, <https://doi.org/10.1134/S2070050415010122>.
- [24] D.-Y. Kim, Y. Nishiyama, M. Wada, S. Kuga, High-yield Carbonization of Cellulose by Sulfuric Acid Impregnation, 2001.
- [25] Y. Habibi, L.A. Lucia, O.J. Rojas, Cellulose nanocrystals: chemistry, self-assembly, and applications, *Chem. Rev.* 110 (2010) 3479–3500, <https://doi.org/10.1021/cr900339w>.
- [26] J. Shokri, K. Adibki, Application of cellulose and cellulose derivatives in pharmaceutical industries, in: *Cellul. - Medical, Pharm. Electron. Appl., InTech*, 2013, <https://doi.org/10.5772/55178>.
- [27] L. Pang, Z. Gao, H. Feng, S. Wang, Q. Wang, Cellulose based materials for controlled release formulations of agrochemicals: a review of modifications and applications, *J. Contr. Release* 316 (2019) 105–115, <https://doi.org/10.1016/j.jconrel.2019.11.004>.
- [28] I. Sayed Yahia, M. Shkir, S. Mohamed Abdel Salam Keshk, Physicochemical properties of a nanocomposite (graphene oxide-hydroxyapatite-cellulose) immobilized by Ag nanoparticles for biomedical applications, *Results Phys.* (2020) 102990, <https://doi.org/10.1016/j.rinp.2020.102990>.
- [29] C. Calvino, N. Macke, R. Kato, S.J. Rowan, Development, processing and applications of bio-sourced cellulose nanocrystal composites, *Prog. Polym. Sci.* (2020) 101221, <https://doi.org/10.1016/j.progpolymsci.2020.101221>.
- [30] N.S. Sharif, H. Ariffin, Cellulose nanofibrils for biomaterial applications, in: *Mater. Today Proc.*, Elsevier Ltd, 2019, pp. 1959–1968, <https://doi.org/10.1016/j.matpr.2019.06.074>.
- [31] S. Keshipour, A. Kamran, Reduction of Nitroaromatics to Amines with Cellulose Supported Bimetallic Pd/Co Nanoparticles, 2018.
- [32] D. dan Li, J. wei Zhang, C. Cai, Chemoselective hydrogenation of nitroarenes catalyzed by cellulose-supported Pd NPs, *Catal. Commun.* 103 (2018) 47–50, <https://doi.org/10.1016/j.catcom.2017.09.024>.
- [33] C.S. Couto, L.M. Madeira, C.P. Nunes, P. Araújo, Hydrogenation of nitrobenzene over a Pd/Al₂O₃ catalyst - mechanism and effect of the main operating conditions, *Chem. Eng. Technol.* 38 (2015) 1625–1636, <https://doi.org/10.1002/ceat.201400468>.
- [34] Z. Wang, H. Liu, L. Chen, L. Chou, X. Wang, Green and facile synthesis of carbon nanotube supported Pd nanoparticle catalysts and their application in the hydrogenation of nitrobenzene, *J. Mater. Res.* 28 (2013) 1326–1333, <https://doi.org/10.1557/jmr.2013.101>.
- [35] V. Hajdu, Á. Prekob, G. Muránszky, I. Kocserha, Z. Kónya, B. Fiser, B. Viskolcz, L. Vanyorek, Catalytic activity of maghemite supported palladium catalyst in nitrobenzene hydrogenation, *React. Kinet. Mech. Catal.* 129 (2020) 107–116, <https://doi.org/10.1007/s11144-019-01719-1>.
- [36] R.M. Mironenko, O.B. Belskaya, Y.G. Kryazhev, T.I. Gulyaeva, V.A. Likhobobov, Palladium hydrogenation catalysts prepared using porous carbon materials derived from poly(vinyl chloride), in: *AIP Conf. Proc.*, American Institute of Physics Inc., 2019, 020005, <https://doi.org/10.1063/1.5122904>.
- [37] F. Haber, Gradual electrolytic reduction of nitrobenzene with limited cathode potential, *Z. Elektrochem.* 4 (1898) 506.
- [38] C.S. Couto, L.M. Madeira, C.P. Nunes, P. Araújo, Commercial catalysts screening for liquid phase nitrobenzene hydrogenation, *Appl. Catal. Gen.* 522 (2016) 152–164, <https://doi.org/10.1016/j.apcata.2016.04.032>.
- [39] C. Wang, F. Yang, W. Yang, L. Ren, Y. Zhang, X. Jia, L. Zhang, Y. Li, PdO nanoparticles enhancing the catalytic activity of Pd/carbon nanotubes for 4-nitrophenol reduction, *RSC Adv.* 5 (2015) 27526–27532, <https://doi.org/10.1039/c4ra16792a>.
- [40] Á. Prekob, G. Muránszky, Z.G. Hutkai, P. Pekker, F. Kristály, B. Fiser, B. Viskolcz, L. Vanyorek, Hydrogenation of nitrobenzene over a composite catalyst based on zeolite supported N-doped carbon nanotubes decorated with palladium, *React. Kinet. Mech. Catal.* 125 (2018) 583–593, <https://doi.org/10.1007/s11144-018-1481-2>.